Wave Modeling Demonstration in EFDC+: Comparing SWAN to Internal SMB for Wave-Driven Sediment Transport

DSI, LLC
EFDC+ Technical Document

July 10, 2026

1 Introduction

Waves matter for sediment transport. The orbital motion of waves near the bed greatly increases bottom shear stress, mobilizing sediment that currents alone would leave in place, while wave–driven setup and radiation–stress gradients generate nearshore currents. EFDC+ therefore offers users a choice of wind–wave forcing:

- **SWAN** (Simulating WAves Nearshore)–a widely used, third–generation *spectral* wave model that EFDC+ reads through a file–based linkage [1, 2]; and
- **SMB**–an internal, *empirical* wind–wave generator based on the Sverdrup–Munk–Bretschneider / Shore Protection Manual fetch–growth relations [4].

This article runs both methods on the same problem to show that EFDC+ handles either forcing transparently within a coupled hydrodynamic and sediment–transport simulation. Along the way, we contrast how the two models compute wave properties, quantify the resulting differences from model output, and recognized the limitations encountered when SWAN is pushed to a laboratory scale far smaller than its intended coastal domain.

2 How SWAN and SMB Compute Wave Properties

The two models represent fundamentally different classes of wave model. The distinction is not merely numerical, it shapes which physics each can and cannot capture. For more computation details for both wind forcings and wave action calculation within EFDC+, please refer to the EFDC+ theory documet version 12 section 2.2.3 and 2.2.4 [10].

2.1 SWAN: Phase-Averaged Spectral Wave Model

SWAN evolves the full two–dimensional wave *spectrum* $E(\sigma, \theta)$ (energy distributed over frequency σ and direction θ) by solving the spectral action–balance equation, with the physics represented by explicit source terms [1, 2]:

- **Wind input.** Wind stress (via a drag law, $u_*^2 = C_d U_{10}^2$) feeds energy into the spectrum; in the Komen formulation the exponential growth rate scales with the ratio of wind speed to wave phase speed, u_*/c [3].

- **Whitecapping** dissipates steep, short waves.
- **Quadruplet wave–wave interactions** transfer energy toward lower frequencies, downshifting the spectral peak as the sea develops.
- **Triad interactions, bottom friction, and depth–induced breaking** reshape and limit the spectrum in shallow water.

SWAN then *diagnoses* the familiar wave parameters as moments of the computed spectrum: significant wave height $H_s = 4\sqrt{m_0}$ (with m_0 the total spectral energy), peak and mean periods, wavelength from the dispersion relation $\sigma^2 = gk \tanh(kh)$, and direction and spreading from the directional distribution. Critically, SWAN *propagates* this spectrum across the grid, so it represents refraction, shoaling, and the sheltering of the lee of the bar.

2.2 SMB: Empirical, Parametric Model

The SMB method predicts integrated wave parameters *directly* from wind speed, fetch, and depth using empirical growth curves derived from dimensional analysis and field data [4, 5]. In EFDC+'s internal implementation, fetch is computed for each cell over a set of directional sectors, and the significant wave height and period follow depth–limited tanh relations; the wavelength is obtained from the dispersion relation and the wave direction is set equal to the wind direction. There is no spectrum, no spatial propagation, and no explicit wave–wave interaction.

2.3 Side–by–Side Summary

Aspect	**SWAN (spectral)**	**SMB (empirical)**
Coupled to EFDC+	One-way coupling	Fully coupling
Representation	Full 2-D spectrum $E(\sigma, \theta)$	Single H_s, T_p per cell
Governing model	Spectral action balance (iterative)	Algebraic fetch–growth curves
Physics	Explicit wind input, whitecapping, quadruplets, triads, friction, breaking	Empirical growth (no explicit source terms)
Fetch	Implicit (energy propagates across the grid)	Explicit per–cell fetch
Propagation	Yes: refraction, shoaling, sheltering	None (each cell independent)
Direction	Computed (spreading, refraction)	Equal to wind direction
Cost	High (spectral solve)	Low (per–cell algebra)

Table 1: Conceptual comparison of the SWAN and SMB wind–wave models.

Unlike the internal SMB wave model, SWAN is not fully coupled with EFDC+. Instead, SWAN is run separately from EFDC+, using either the same model grid or over a larger SWAN model domain where EFDC+ model resides in. The default option EEMS uses are the same model grid, bathymetry, and forcing conditions as the EFDC+ model to generate wave fields. The resulting wave parameters, such as significant wave height, wave period (or frequency), wave direction and wave dissipation energy, are then imported into the EFDC+ hydrodynamic model and remain as-is throughout the simulation. EFDC+ uses these prescribed wave fields to compute wave-induced processes, including bottom shear stress and sediment resuspension, but there is no dynamic feedback from the hydrodynamic or sediment transport models to SWAN during the simulation.

3 Test Case

The test is an idealized, flume–scale domain (∼15 m cross–shore by 16 m alongshore, 0.25 m cells, still–water depths of roughly 0.07–0.15 m) featuring an alongshore–periodic sand bar with regular openings (a "rip–channel" bathymetry). A spatially uniform onshore wind generates waves that shoal and break over the bar; the resulting wave–driven bed shear and circulation transport non–cohesive sediment. Two companion EFDC+ models were built that are identical except for the wind–wave forcing:

- **SWAN–forced wind wave model**
- **SMB–forced wind wave model**

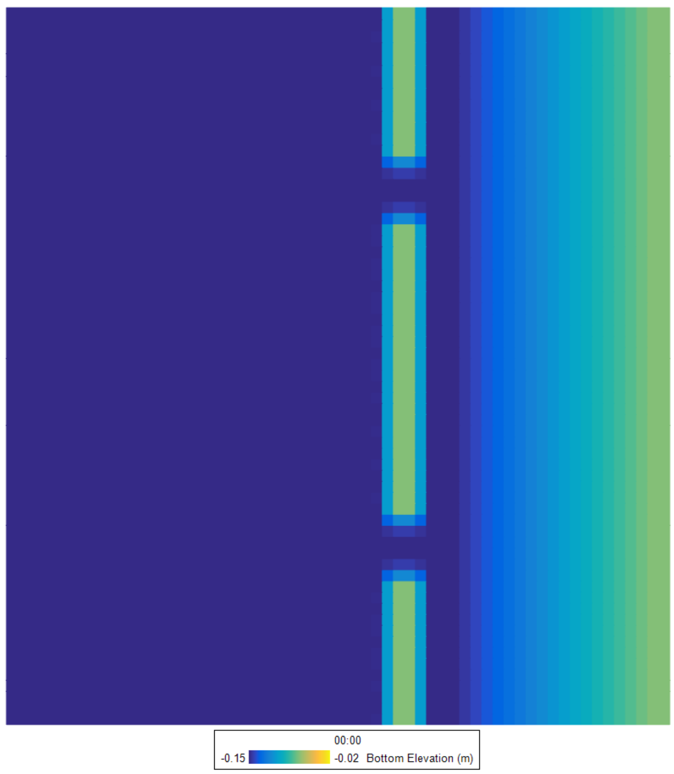

Figure 1: Initial bathymetry of the rip–channel test domain at $t = 0$.

The domain (Fig. 1) combines a flat offshore region, a series of shore–parallel bar segments separated by regular openings, and a shoaling beach face.

3.1 Model Configuration

Table 2 summarizes the key configuration shared by both runs. The two models are identical except for the wind–wave forcing.

Domain and grid	
Domain size	$\sim$15 m (cross–shore) $\times$ 16 m (alongshore)
Horizontal cells	60 $\times$ 64 at 0.25 m resolution
Bathymetry	Alongshore–periodic sand bar with regular openings ("rip–channel"); still–water depths $\approx$ 0.07–0.15 m
Vertical resolution	8 standard sigma layers (water column); 2 sediment bed layers
Forcing	
Wind	Spatially uniform, constant in time 15m/s; shore–normal (onshore)
Wave forcing (two runs)	**SWAN** (external 3rd–generation spectral) vs. **SMB** (internal empirical)
Water density / gravity	$\rho = 1025\,\mathrm{kg\,m^{-3}}$; $g = 9.81\,\mathrm{m\,s^{-2}}$
Sediment transport	
Module	Original EFDC ("SedOrg")
Classes	4 non-cohesive (quartz sand), D_{50} = 100–350 μm, SG 2.65
Load	Suspended (Garcia–Parker) + bed load (Engelund–Hansen)
Bed shear / roughness	Standard aggregate bed shear; roughness from local D_{50}
Morphology	Morphologic feedback enabled (bed updates)
Timing	
Duration / output	4 hours; results every 5 minutes (SWAN and EFDC+)
Sediment start	0.1 days ($\approx$2.4 hours); $\sim$1.6 hours of morphological evolution
Sediment time step	1 s

Table 2: Model setup. Both models share this configuration; only the wind–wave forcing differs.

3.2 SWAN Model Configuration

Because the SWAN domain interacts with open lateral boundaries (discussed in Section 5), the SWAN grid was *extended three times in the alongshore direction*, and only the *middle section* of the SWAN solution was extracted and mapped onto the EFDC+ grid. In addition, because the idealized geometry is symmetric and the incident wind is exactly shore–normal, the wave *direction* produced by SWAN contained a small, numerical bias; for this controlled demonstration the wave direction was therefore *manually overridden to shore–normal (*0°*)*. We return to the rationale and trade–offs of these choices in Section 5.

3.3 Sediment Transport Configuration

Both models share an identical EFDC+ sediment setup; only the wind–wave forcing differs. The water column is resolved with **8 standard sigma layers**, and the bed with **2 sediment bed layers** (the EFDC+ dialog reports "4," which additionally counts 2 active sediment–to–water–column interface layers). Sediment is simulated with the **original EFDC sediment–transport module** (the "SedOrg" approach, not SEDZLJ) [9], using **four non-cohesive (quartz sand) size classes** and no cohesive fraction. Both **suspended load** (Garcia–Parker) and **bed load** (Engelund–Hansen) are active, the bed shear is computed with the standard aggregate option, and the non-cohesive bed roughness is taken from the local D_{50}. The bed uses active–parent (armoring) layering with a 0.01 m active layer, and hard–bottom limits are imposed via `BEDMAP.INP` to exclude open boundary cells from sediment transport processes. **Morphologic feedback is enabled**, so the simulated erosion and deposition update the bed elevation and feed back on the hydrodynamics. Class properties are summarized in Table 3.

Class	D_{50} (μm)	Settling vel. (mm s^{-1})	Specific gravity	Critical shear τ_{cr}/ρ (m^2 s^{-2})	Critical Shields θ_{cr}
NonCoh1	100	8.99	2.65	1.535×10^{-4}	0.0949
NonCoh2	150	16.23	2.65	1.535×10^{-4}	0.0633
NonCoh3	250	35.14	2.65	1.740×10^{-4}	0.0430
NonCoh4	350	51.93	2.65	1.964×10^{-4}	0.0347

Table 3: Properties of the four non-cohesive sediment classes. The critical shear is listed in kinematic form (τ_{cr}/ρ); multiplying by $\rho = 1025\,\mathrm{kg\,m^{-3}}$ gives $\approx$ 0.16–0.20 N m^{-2}.

Both the SWAN wave computation and the EFDC+ hydrodynamic/sediment computation run for **4 hours**, with output every **5 minutes**. The sediment time step is 1 s, assures the the stability and convergence of the bed updates along with 5 minutes wave-forcing. **Morphological computation begins at 0.1 days (≈2.4 hours)**: the first 2.4 hours spin up a quasi–steady wave and current field, after which bed change is computed over the final ∼1.6 hours. This "cold–start" delay ensures the bed responds to a fully developed wave and current field rather than to start–up transients.

4 Results and Discussion

We present the wave field, the wave–induced bed shear (with a quantitative breakdown of the difference between the two forcings), and finally the circulation and bed–change response.

4.1 Wave Field

Figures 2 and 3 compare the wave height fields. After extending the SWAN upper frequency limit to capture the young, high–frequency wind sea (Section 5), both models produce wave heights of broadly similar order (growing from near zero at the offshore, windward edge to a few centimeters toward shore).

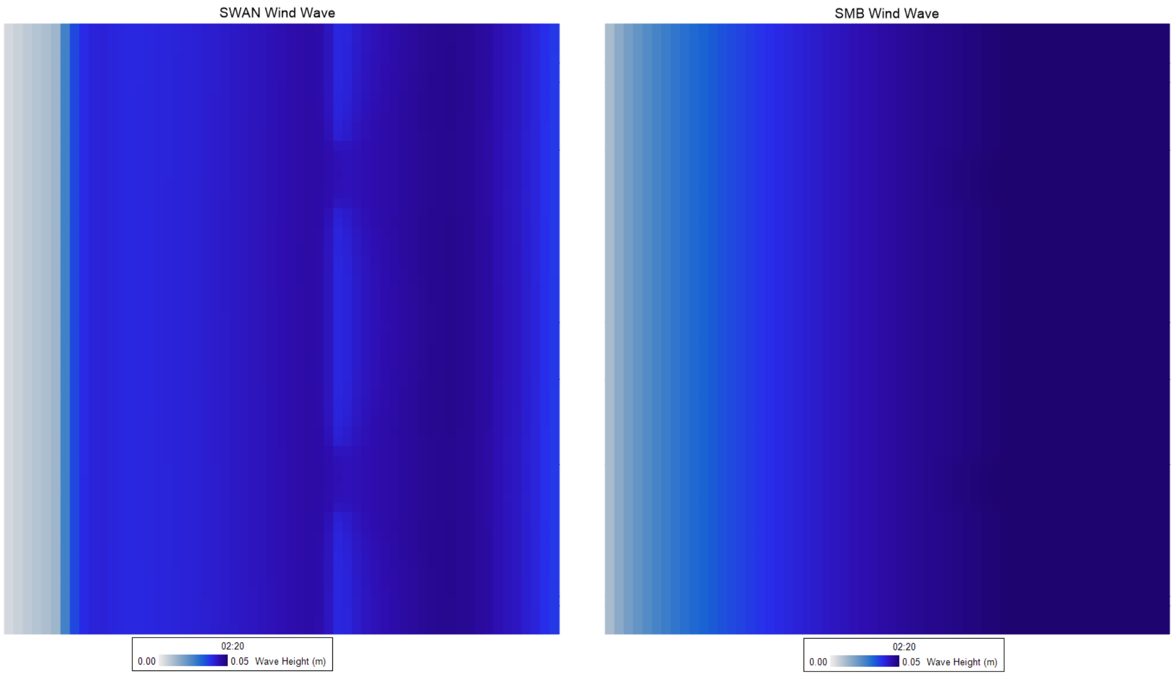

Figure 2: Significant wave height: SWAN (left) vs. SMB (right).

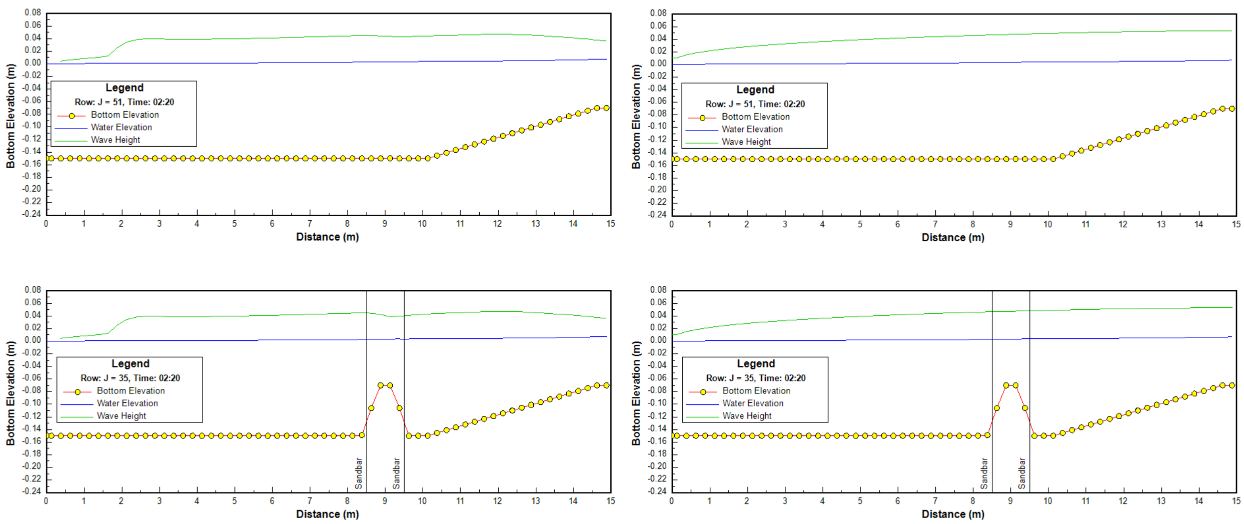

Figure 3: Cross–shore wave transformation through an opening (top) and a bar (bottom), SWAN (left) vs. SMB (right).

The differences are in the *spatial structure*. The SMB field is smooth and nearly alongshore–uniform, because SMB computes each cell's wave height independently from its local fetch and depth, with no spatial propagation. The SWAN field shows more alongshore structure—the bar segments and openings modulate the waves through shoaling, breaking, and refraction, processes only a propagating spectral model represents. The cross–shore profiles (Fig. 3) confirm both models grow the wave height with fetch and respond to the bar, while SWAN resolves the local transformation over the bar crest.

4.2 Wave–induced Bed Shear Stress

The most consequential difference appears in the wave–induced bed shear stress (Fig. 4): the SMB forcing produces *substantially higher* bed shear than SWAN. We examine cell–level output at a representative nearshore cell ($I, J = 61, 35$; depth ≈ 0.077 m), summarized in Table 4.

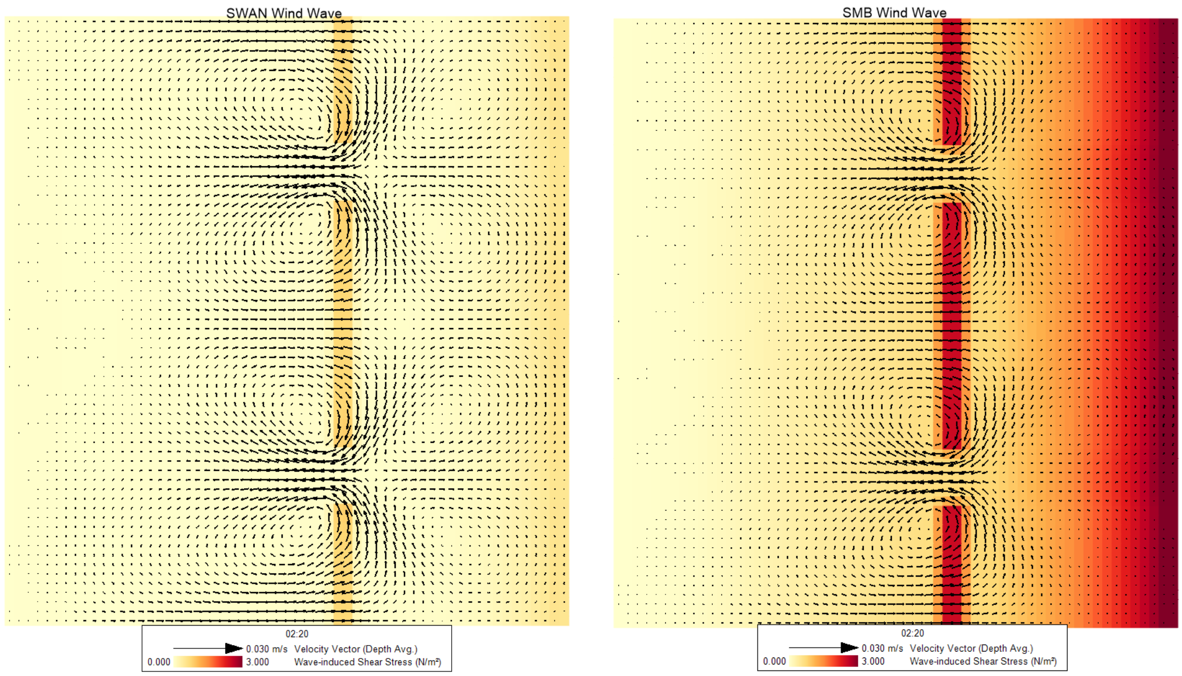

Figure 4: Wave–induced bed shear stress and circulation, SWAN (left) vs. SMB (right).

Quantity	SWAN	SMB	SMB/SWAN
Wave height H (m)	0.0374	0.0532	1.42
Wave period T (s)	0.541	0.718	1.33
Wavelength L (m)	0.285	0.560	1.97
Depth h (m)	0.077	0.076	$\approx$1.0
Relative depth kh	1.70	0.85	0.50
$\sinh(kh)$	2.66	0.96	0.36
Near–bed orbital vel. U_{orb} ($\mathrm{m\,s^{-1}}$)	0.082	0.243	2.96
Wave–induced bed shear ($\mathrm{N\,m^{-2}}$)	0.531	2.992	5.64

Table 4: Cell–level wave parameters at $I, J = 61, 35$ (t = 02:20). U_{orb} computed as $\pi H/[T \sinh(kh)]$.

Two properties differ, and both raise the SMB bed shear:

1. **Bottom penetration** The SMB wavelength is nearly double SWAN's (0.56 vs. 0.28 m), so the relative depth kh drops from 1.70 to 0.85. Near–bed orbital velocity scales with $1/\sinh(kh)$, a strongly nonlinear factor: the smaller kh alone boosts the orbital velocity by $\sim\times 2.8$. Longer waves simply reach the bed far more effectively.

2. **Wave height** The SMB wave height is $\sim$42% larger here, and height enters the orbital velocity linearly ($\times 1.42$).

Combining $(1.42 \times \frac{0.541}{0.718} \times \frac{2.66}{0.96} \approx 2.96)$ reproduces the $\sim$3× larger orbital velocity (0.24 vs. $0.08\,\mathrm{m\,s^{-1}}$). Bed shear scales with the *square* of orbital velocity, which would imply $\sim$8.8×; the observed ratio is $\sim$5.6× because the friction (drag) coefficient *decreases* with the larger orbital excursion of the SMB waves, partially offsetting the increase.

The key lesson for users: **comparable wave heights do not imply comparable bed shear–relative depth kh (bottom penetration) is decisive, and it depends nonlinearly on wavelength**. The difference in wave period expressed in seconds (0.18 s here) understates the effect, because shear responds to kh through $\sinh(kh)$. This is also the downstream consequence of resolving SWAN's young, high–frequency sea (Section 5): doing so raised SWAN's wave height but shortened its waves, reducing their effectiveness at the bed relative to the longer–period SMB sea.

4.3 Circulation and Bed Morphological Response

Both forcings drive the expected **rip-current circulation** (Figs. 4 and 5): coherent circulation cells form on either side of each opening, with flow converging behind the bars and exiting seaward through the gaps–the signature of bar/rip current hydrodynamics. That EFDC+ reproduces this circulation under *either* wave forcing is the central demonstration of this article.

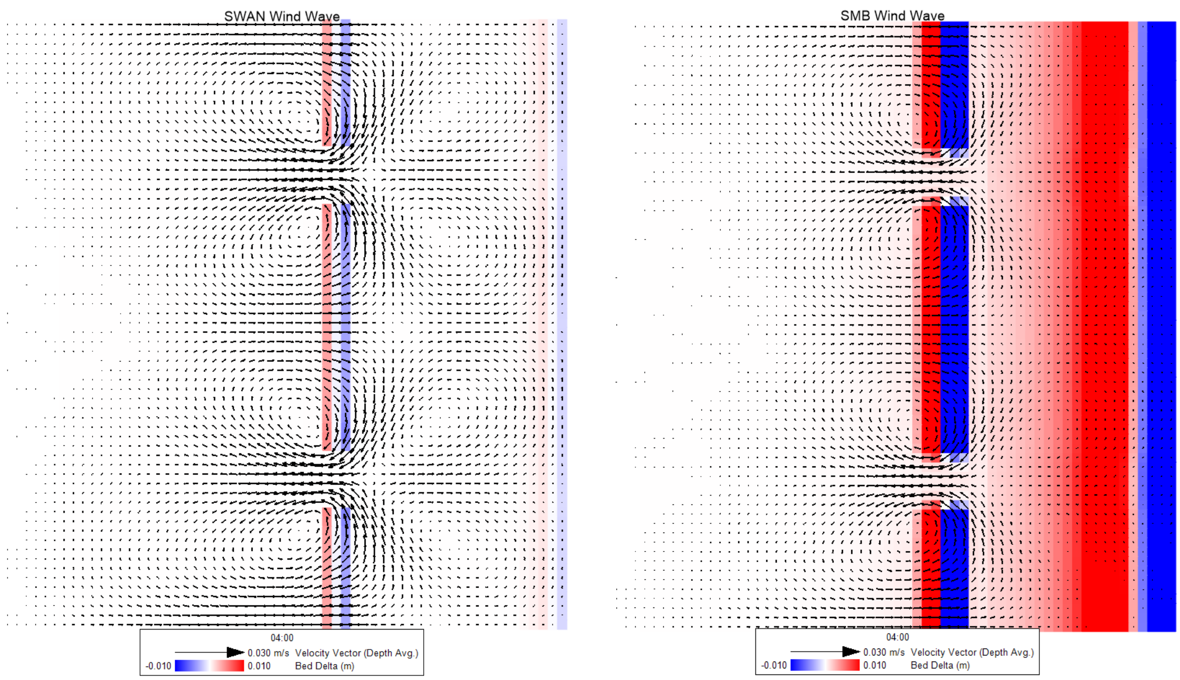

Figure 5: Bed–elevation change (Bed Delta) and circulation at the end of the simulation, SWAN (left) vs. SMB (right).

The bed–change magnitudes differ markedly. Consistent with its much higher bed shear, the **SMB run drives substantially larger erosion and deposition** (Fig. 5, right), whereas the SWAN run (left) produces a far more subdued bed response. Both, however, organize the bed change into the *same qualitative pattern* dictated by the rip–cell circulation. The two forcings therefore agree on the *pattern* of wave–driven transport while differing greatly in its *magnitude*, with the difference traceable directly to the bed–shear analysis above.

4.4 Synthesis

The side–by–side results illustrate three points:

1. EFDC+ couples transparently to both an external spectral model (SWAN) and the internal empirical model (SMB), producing coherent wave–driven circulation and sediment transport with either method.

2. Comparable wave heights can still produce very different bed shear: relative depth kh (bottom penetration) and the resulting near–bed orbital velocity are also decisive.

3. The two models agree on the pattern of the rip–cell morphodynamics but differ in magnitude. Because this idealized case is uncalibrated (no measured data), the comparison characterizes model behavior, not accuracy; selecting and calibrating the appropriate forcing for a given site remains essential.

5 Limitations of SWAN in the Test Case

SWAN is a coastal– and shelf–scale model, designed for domains of hundreds of meters to hundreds of kilometers, with many wavelengths across the grid and source terms calibrated against field conditions [1, 5]. Applying it to a ∼15 m flume is outside that regime, and several of its assumptions become strained. We list the effects we encountered, because they are instructive for any user pushing SWAN toward small scales.

1. **Open lateral–boundary contamination.** Where an incident spectrum is not prescribed, SWAN imposes zero incoming energy along the boundary, truncating the obliquely–travelling part of the directional spectrum and skewing wave height and direction in a wedge that penetrates inward-direction more deeply than height. We therefore extended the grid alongshore and analyzed only the middle section.

2. **Directional discretization (banding and a one–sided bias).** The peak wave direction is reported on a discrete directional grid, appearing as 1° bands. In a perfectly symmetric, shore–normal problem the true direction is 0°, but the deterministic tie–break in selecting the peak directional bin (together with the boundary effect above) produced a small, consistent (∼1°) bias. Because EFDC+ uses this direction in the radiation–stress computation, along with the small model domain, even a degree of spurious obliquity drives a spurious alongshore current. For this controlled demonstration we overrode the direction to shore–normal—defensible *only* because the geometry and forcing are provably symmetric, and not appropriate for a genuinely oblique field, where SWAN's computed direction and refraction should be retained.

3. **Spectral (frequency) truncation.** At very short fetch the wind sea is "young" and its spectral peak sits at high frequency. A default upper frequency that is too low truncates the peak and under–predicts wave height; extending it restored a more physical height but shortened the dominant waves. As Section 4.2 shows, short waves contribute little to near–bed orbital velocity, so a higher H_s does not necessarily imply higher bed shear.

4. **Phase–averaged physics:** SWAN is phase–averaged and only utilizes a phase-decoupled refraction-diffraction approximation For a laboratory bar/opening geometry, the diffraction and velocity skewness that drive sediment transport are not fully represented; a phase–resolving model would be required for those details.

5. **Gravity–wave assumption.** SWAN's dispersion is purely gravitational and cannot represent capillary–gravity effects relevant at centimeter scales.

These limitations reflect the extreme *scale* of this test, not deficiencies of SWAN within its intended domain. In a field–scale, broad–banded, properly nested application, boundary buffering and the natural directional spread render most of them negligible [8, 6]. The SMB model, being empirical and unidirectional, sidesteps the directional and boundary issues entirely-at the cost of representing none of the wave transformation over the bar.

6 Takeaways for EFDC+ Users

- EFDC+ couples cleanly to *both* an external spectral wave model (SWAN) and an internal empirical model (SMB) within the same coupled hydrodynamic–sediment framework; the choice is the user's.
- Use **SMB** for efficient, fetch–limited wind–wave estimates in simple geometries where wave transformation over features is not central.
- Use **SWAN** when refraction, shoaling, breaking, and wave transformation over complex bathymetry matter-accepting its higher computation cost and the configuration care it requires.
- When applying **SWAN** near its scale limits, buffer the lateral boundaries, verify the frequency range captures the spectral peak, and interpret wave direction critically.
- Wave induced bed shear stress depends on the bed orbital velocity. While wave height is one of the major factor, it is not the only wave parameters that affect wave induced bed shear stress.

References

[1] Booij, N., Ris, R.C., & Holthuijsen, L.H. (1999). A third-generation wave model for coastal regions, 1. Model description and validation. *Journal of Geophysical Research*, 104(C4), 7649–7666.

[2] The SWAN Team. *SWAN User Manual* and *SWAN Scientific and Technical Documentation* (Cycle III). Delft University of Technology.

[3] Komen, G.J., Cavaleri, L., Donelan, M., Hasselmann, K., Hasselmann, S., & Janssen, P.A.E.M. (1994). *Dynamics and Modelling of Ocean Waves*. Cambridge University Press.

[4] U.S. Army Corps of Engineers (1984). *Shore Protection Manual*. Coastal Engineering Research Center, Vicksburg, MS. (Sverdrup–Munk–Bretschneider / depth–limited fetch–growth relations.)

[5] Holthuijsen, L.H. (2007). *Waves in Oceanic and Coastal Waters*. Cambridge University Press.

[6] Tolman, H.L. (2002). Alleviating the garden sprinkler effect in wind wave models. *Ocean Modelling*, 4(3–4), 269–289.

[7] Booij, N., & Holthuijsen, L.H. (1987). Propagation of ocean waves in discrete spectral wave models. *Journal of Computational Physics*, 76(1).

[8] Dietrich, J.C., Zijlema, M., et al. (2013). Limiters for spectral propagation velocities in SWAN. *Ocean Modelling*, 70, 85–102.

[9] Hamrick, J.M. (1992). *A Three-Dimensional Environmental Fluid Dynamics Computer Code (EFDC): Theoretical and Computational Aspects*. Virginia Institute of Marine Science.

[10] DSI, LLC. *EFDC+ Theory Document Version 12* (2024).